GEOPHYSICAL RESEARCH LETTERS, VOL. 22, NO. 22, PAGES 3019-3022, NOVEMBER 15, 1995

Mapping thermospheric winds in the auroral zone

M. Conde and R.W. Smith
Geophysical Institute, University of Alaska

Abstract. A new all-sky imaging Fabry-Perot (ASIFP) spectrometer has been developed for ground-based mapping of upper atmospheric wind and temperature fields in the auroral zone . Although several other ASIFP spectrometers exist for atmospheric studies [Rees et al., 1984; Sekar et al., 1993; Biondi et al., 1995] these instruments have all operated with etalons of fixed optical gap, a method potentially subject to errors in the presence of auroral intensity gradients. In this instrument the etalon plate spacing is scanned periodically over one order of interference and each photon detected is assigned to a wavelength interval which is determined from both its arrival location on the detector and the etalon plate spacing prevailing at the detection time. Spectra accumulated this way are not distorted by spatial intensity gradients. Preliminary λ630 nm observations were made during the winter of 1994/95 from Poker Flat Research Range, Alaska. To illustrate some of the features we have observed in this study we present line-of-sight wind estimates derived for the night of December 7, 1994. The background wind matches averages presented previously by Sica et al. [1986] and is consistent with winds driven principally by momentum deposition from ionospheric plasma convection through ion-drag. Smaller scale curvature and divergence features are also discernable and are discussed.

Introduction

There has been considerable experimental and theoretical interest in the small-scale structure of thermospheric wind and temperature fields at auroral latitudes. Observations suggest thermospheric wind and temperature structures exist with length scales comparable to the ~800 km distance visible from a single ground station, or smaller. Ground-based instruments viewing in opposite directions often give results differing by more than the measurement uncertainty, as shown for example by Hernandez and Roble [1978]. A series of papers [Rees et al., 1984; Batten et al., 1988; Batten and Rees, 1990] have described observations of horizontal wind fluctuations with small spatial scales (100-200 km) and amplitudes of the order of 150 ms^{-1} obtained with an ASIFP spectrometer observing at λ630 nm in the auroral zone at Kiruna, Sweden. Eastes et al. [1992] have presented a study of auroral arc crossings by Dynamics Explorer 2. Zonal winds, vertical winds, and temperatures were recorded with spatial resolutions of 60-120 km. Zonal wind features were observed with large amplitudes (up to 600 ms^{-1}) and were clearly associated with arc crossings. After restricting the data to crossings of a long lived, isolated, arc suitable for model comparisons, they found wind maxima in all three components (zonal, meridional and vertical) which significantly exceeded the model predictions.

Several two-dimensional models with high spatial resolution have been used to examine the atmospheric response to energy and momentum sources associated with auroral arcs [St. Maurice and Schunk, 1981; Fuller-Rowell, 1985; Lyons and Walterscheid, 1985; Walterscheid et al., 1985; Chang and St.-Maurice,1991; Walterscheid and Lyons, 1992]. These simulations varied in detail but all produced large zonal winds of hundreds ms^{-1} after several hours of simulated arc presence. The Walterscheid et al. [1985] and Walterscheid and Lyons [1992] simulations both predicted strong differences between zonal winds to the north and to the south of the arc.

Paper number 95GL02437
0094-8534/95/95GL-02437$03.00

Instrument Description

The instrument used here is based on a 100 mm aperture capacitance-stabilized Fabry-Perot etalon, the plates of which are piezoelectrically scannable in spacing over approximately 1.5 orders of interference (at λ630 nm) about a nominal 20 mm gap. Skylight is coupled into the etalon through an all-sky lens and optical relay system which maps an approximately 75° half-angle field-of-view onto 5 orders of interference at the etalon. Interference fringes formed by the etalon are conjugate with the sky. The sky, modulated by this fringe pattern, is re-imaged onto an imaging photon detector (IPD) after first passing through a narrow-band interference filter.

The key difference between this and previous ASIFP systems is that here the etalon plates are rapidly scanned in separation. For each individual photon recorded by the IPD a spectral bin is calculated using both its detected position and the plate spacing prevailing at detection time. The plates scan through one whole order of interference in 128 steps or "channels" every seven seconds.

Prior to sky observations the instrument records a calibration map of the detector which encodes, for each pixel location, the etalon gap required to maximize the transmitted intensity at that pixel of a monochromatic source at the nominal observing wavelength. The appropriate spectral channel to assign to a photon detection during sky observations is then given by the differ-

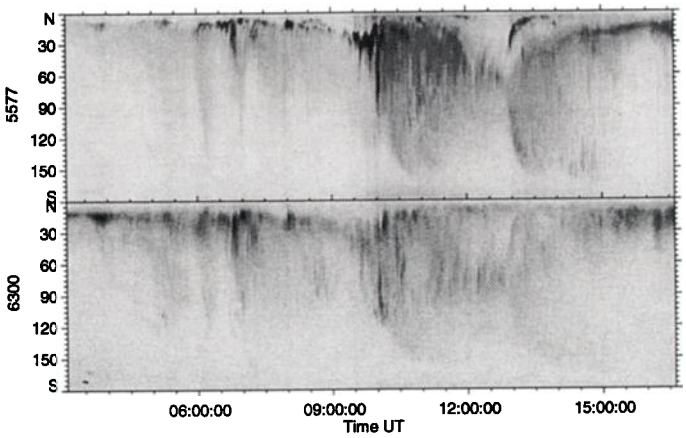

Figure 1. Poker Flat meridian scanning photometer data for 07-Dec-1994. These panels indicate airglow and auroral emission intensities at λ557.7 nm (top) and λ630.0 nm (bottom) measured along the magnetic meridian as functions of universal time. The Y-axis indicates viewing angle in degrees along the magnetic meridian, with 0 corresponding to the north horizon and 180 to the south horizon. The intensity scale is linear, with black corresponding intensities of 8 kilo-Rayleighs or more for the upper panel and 2.2 kR or more for the lower panel.

ence between the current plate spacing and that spacing at which transmission maximizes for the detection location. Each detected photon is added to the total for its allocated spectral channel so that, at the end of each scan through one order in plate spacing, the photon totals represent a spectrum spanning one free spectral range in wavelength.

Since spectral accumulation is valid for any subset of the detector's pixels it is possible to divide the detector into any number of zones, of arbitrary shape(s), and accumulate an independent spectrum for each zone. Here, we have allocated a total of 25 zones mapping onto the sky as sectors of four concentric, annular, rings centered about the zenith. The ring edges were spaced uniformly in zenith angle, with the outermost being at 75°. The rings contained 1,4,8 and 12 sectors respectively.

Other ASIFP spectrometers operate with a fixed plate spacing and form static Fabry-Perot fringes optically conjugate with the sky. In this configuration the shapes of the Fabry-Perot fringes are modulated by variations across the sky of both the intensity and spectral content of the emission. The intensities of aurorally-excited emissions may vary significantly over angular distances comparable to the widths of the Fabry-Perot fringes projected onto the sky. For example, photometer data for our observing night are shown in Figure 1 and illustrate typical spatial brightness variations during moderate auroral activity. These would, presumably, distort spectra inferred from static fringe patterns and may ultimately appear as small-scale artifacts in derived wind fields. Our instrument is not subject to this potential source of error. A complete description of it is in preparation and will be presented in a future paper.

Line-of-Sight Winds on December 7, 1994

The prototype version of this instrument was operated during the winter of 1994/95 observing at λ630 nm. Twenty nights of good data were obtained after allow-

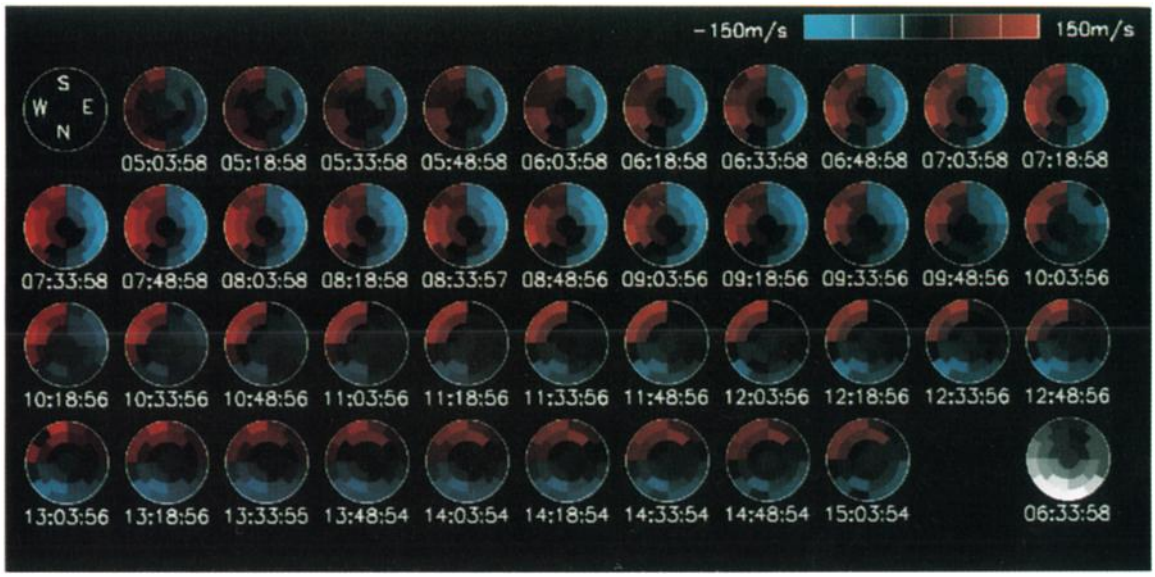

Figure 2. Sky maps of line-of-sight wind speeds, with blue indicating approaching and red indicating receding flows. Higher speeds are indicated by brighter colors. These sky maps use the all-sky camera orientation convention, as indicated. The outer edge of each image corresponds to a zenith angle of approximately 75°. Central times (UT) are indicated for each exposure period. Magnetic midnight is at around 1120 UT. The grey-scale sky map in the lower right corner shows an example of the λ630 nm intensities recorded during one exposure, centered around 0634 UT. The brightest λ630 nm intensity shown corresponds to approximately 2 kilo-Rayleighs; brightness enhancement due to an auroral arc lying north of Poker Flat is apparent.

ing for cloud and periods of instrument development. Here we present line-of-sight winds obtained from one night, December 7, 1994. This was a magnetically disturbed period, with K_p generally between 3 and 4 in the preceding 24 hours. K_p dropped to 2+ between 0900 and 1200 UT. We have not yet derived thermospheric temperatures from our ASIFP data, however a conventional FPI at Poker Flat was also observing at λ630 nm, mostly in the zenith. Temperatures recorded by it lie between 600 and 700 K for this night, with a weak cooling trend amounting to about 50 K over the observing period. The data show no discernable heating events.

Figure 2 shows sky maps of line of sight wind speeds. We have limited our figure to line-of-sight wind components, since this requires no assumptions about the underlying velocity field, in contrast to presentation of derived vectors [Batten et al., 1988]. However, in our discussion below, we interpret these data in terms of the horizontal winds we consider most likely to have produced the observed line-of-sight pattern. For example, a uniform horizontal wind would yield a non-uniform plot, with line-of-sight speeds of zero in the center and with maxima near the edges at two opposing azimuths. This interpretation is not unique, since a vortex flow centered on the instrument could be added with no change observable in the line-of-sight components.

For the majority of spectra, line-of-sight wind estimates were obtained with statistical uncertainties of a few ms^{-1}. However, during this study, we used an IPD at room temperature and with several regions of low sensitivity on its photocathode. These regions yielded low signal-to-noise ratio spectra in the absence of aurora, with corresponding wind uncertainties of many tens of ms^{-1} at times. Because of these uncertainties only the uniform wind and first-order curvature and divergence departures from uniformity are significant. Further, 15-minute data from this night have been smoothed in time with a 30 minute boxcar window.

Early in the evening winds were blowing from geomagnetic east to west at $\sim$100 ms^{-1}, consistent with forcing by sunward plasma flow in the dusk convection cell. Over the next 2.5 hours this westward flow strengthened so that by 0800 it had reached $\sim$180 ms^{-1}. After 0800 wind speeds generally declined, dropping to just under 100 ms^{-1} at the end of the observations. Starting at around 0848 the approaching flow rotated to come from the south-east whereas receding flow continued to be directed westward. Then, between about 1003 and 1118 the approaching flow turned, so that by 1118 the wind was coming from the north-west. During this time the direction of receding flow also rotated, but only through about 45 degrees such that by 1118 it was blowing to the magnetic south-west. Between about 1103 and 1233 the strongest approaching and receeding flows were not seen in opposite viewing azimuths. We interpret this as a curved velocity field, since this is the simplest perturbation from uniformity which would yield these line-of-sight components.

The flow "re-arrangement" between about 1003 and 1118 followed an auroral breakup north of Poker Flat, as indicated by the meridian-scanning photometer (MSP) record in Figure 1. A nearby all-sky video camera at Eagle, Alaska, recorded active auroral forms in the northern half of the sky between 0930 and 1000 U.T., followed by diffuse, pulsating, aurora for the remainder of our observing period. However, on a planetary scale, magnetic activity declined during the three hours from 0900 to 1200, since K_p went from 3+ to 2+ . By 1233 curvature of the velocity field began to weaken and by 1333 nearly uniform flow had been re-established, now directed anti-sunward.

Discussion

Sica et al. [1986] presented average thermospheric wind measurements made during solar maximum with a Fabry-Perot spectrometer at College, Alaska, about 40 km from Poker Flat. This was a narrow-field instrument viewing in magnetic meridional and zonal directions, as well as in the geographic zenith. By considering just the uniform component of our wind field and its variation through the night, we find good agreement in both speed and direction with the Sica et al. averages for moderate magnetic activity. This is despite the 10.7 cm solar radio flux index being only 78 during our observations and having been below 80 throughout the previous month.

MSP data shown in Figure 1 indicate that a quiet arc lay several hundred km north of Poker Flat during the first half of our observing period. Modeling studies cited previously have all predicted that zonal winds of many hundreds of ms^{-1} can be excited within a few hundred km latitude of such an arc. Observed winds were indeed westward early in the evening, and strengthened while the arc was present, although the maximum wind recorded was only $\sim$180 ms^{-1}. Since this arc remained far to the north, enhanced winds which it may have driven would only overlap the northernmost viewing zones, where line-of-sight measurements are insensitive to zonal velocities. Thus, observations of this one arc are not a sensitive test of auroral wind models. The ideal data set for model comparison would include many examples of arcs remaining stable in the zenith for an hour or more. Since stable arcs typically lie north of Poker Flat we anticipate needing many more observations to obtain such a record.

Magnetic midnight at Poker Flat is at about 1120 UT, which corresponds well with the time that we began observing curved flow. Ionospheric convection models, for example those of Heppner and Maynard [1987], suggest plasma flow can indeed be highly curved at this time. Our observations are consistent with a neutral wind curved similarly to Heppner and Maynard's plasma convection models which, for all IMF configurations, predict that an observer in this sector would see

approaching plasma flow when looking north-west and receding flow when looking south west. Although we have only presented one example, similar curvature near magnetic midnight was a common feature in data from the 1993/94 winter. Convection models generally contain more uniform flow in the local time sector immediately after passage of the Harang discontinuity. Again, this is consistent with the observed winds, which gradually lost their curvature after 1230.

Conclusion

A new ASIFP spectrometer capable of ground-based mapping of upper atmospheric wind and temperature fields in the auroral zone has been developed. Its main advantages are insensitivity to spatial intensity gradients and its ability to subdivide the sky into any number of zones of arbitrary shape.

Line-of-sight wind estimates derived for the night of December 7, 1994, show both uniform winds as well as first-order curvature and divergence departures from uniformity. The general character of these features matches average winds presented previously by Sica et al. [1986] and is consistent with winds driven principally by ion-drag. Zonal winds observed while a weak auroral arc lay north of the observatory are consistent with numerical models, but are not a sensitive test of them.

Acknowledgments. This work was supported by NASA grant number NAG5-699 and NSF grant number OPP93-9316163. We thank James Conner of the Geophysical Institute for operating the ASIFP spectrometer on the night presented here. All-sky video tape from Eagle was supplied by Tom Hallinan of the Geophysical Institute and the narrow field FPI at Poker was run in collaboration with Gonzalo Hernandez of the University of Washington.

References

Batten, S., and D. Rees, Thermospheric winds in the auroral oval: observations of small scale structures and rapid fluctuations by a Doppler Imaging System, *Planet. Space Sci.*, *38*, 675-694, 1990.

Batten, S., D. Rees, and D. Wade, Observations of thermospheric neutral winds by the UCL Doppler imaging system at Kiruna in northern Scandinavia, *J. Atmos. Terr. Phys.*, *50*, 861-888, 1988.

Biondi, M. A., D. P. Sipler, M. E. Zipf, and J. L. Baumgardner, All-sky Doppler interferometer for thermospheric dynamics studies, *App. Opt.*, *34*, 1646-1654, 1995.

Chang, C. A., and J.-P. St.-Maurice, Two-dimensional high-latitude thermospheric modeling: a comparison between moderate and extremely disturbed conditions, *Can. J. Phys.*, *69*, 1007-1031, 1991.

Eastes, R. W., T. L. Killeen, Q. Wu, J. D. Winningham, W. R. Hoegy, L. E. Wharton, and G. R. Carignan, An experimental investigation of thermospheric structure near an auroral arc, *J. Geophys. Res.*, *97*, 10539-10549, 1992.

Fuller-Rowell, T. J., A two-dimensional, high-resolution, nested- grid model of the thermosphere 2. Response of the thermosphere to narrow and broad electrodynamic features, *J. Geophys. Res.*, *90*, 6567- 6586, 1985.

Heppner, J. P., and N. C. Maynard, Empirical High Latitude Electric Field Models, *J. Geophys. Res.*, *92*, 4467-4489, 1987.

Hernandez, G., and R. G. Roble, Observations of large-scale thermospheric waves during geomagnetic storms, *J. Geophys. Res.*, *83*, 5531-5538, 1978.

Lyons, L. R., and R. L. Walterscheid, Generation of auroral omega bands by shear instability of the neutral winds, *J. Geophys. Res.*, *90*, 12321-12329, 1985.

Rees, D., A. H. Greenaway, R. Gordon, I. McWhirter, P. J. Charleton, and A. Steen, The Doppler Imaging System: Initial Observations of the Auroral Thermosphere, *Planet. Space Sci.*, *32*, 273-285, 1984.

St. Maurice, J. P., and R. W. Schunk, Ion-neutral momentum coupling near discrete high-latitude ionospheric features, *J. Geophys. Res.*, *86*, 11299-11321, 1981.

Sekar, R., S. Gurubaran, and R. Sridharan, All sky imaging Fabry- Perot spectrometer for optical investigation of the upper atmosphere, *Indian Journal of Radio & Space Physics*, *22*, 197-204, 1993.

Sica, R. J., M. H. Rees, G. J. Romick, G. Hernandez, and R. G. Roble, Auroral Zone Thermospheric Dynamics 1. Averages, *J. Geophys. Res.* , *91*, 3231-3244, 1986.

Walterscheid, R. L., and L. R. Lyons, The neutral circulation in the vicinity of a stable auroral arc, *J. Geophys. Res.*, *97*, 19489-19499, 1992.

Walterscheid, R. L., L. R. Lyons, and K. E. Taylor, The perturbed neutral circulation in the vicinity of a symmetric stable auroral arc, *J. Geophys. Res.*, *90*, 12235-12248, 1985.

M. Conde and R.W. Smith, Geophysical Institute, University of Alaska, 903 Koyukuk Drive, P.O. Box 757320, Fairbanks, Alaska 99775-7320

(received June 12, 1995; accepted July 24, 1995.)